THE ASTROPHYSICAL JOURNAL, 565:L105–L108, 2002 February 1
© 2002. The American Astronomical Society. All rights reserved. Printed in U.S.A.

557 GHz OBSERVATIONS OF WATER VAPOR OUTFLOW FROM VY CANIS MAJORIS AND W HYDRAE

MARTIN HARWIT[1]
511 H Street, SW, Washington, DC 20024-2725
AND
EDWIN A. BERGIN
Harvard-Smithsonian Center for Astrophysics, 60 Garden Street, Cambridge, MA, 02138
Received 2001 September 7; accepted 2001 December 18; 2002 January 11

ABSTRACT

We report the first detection of thermal water vapor emission in the 557 GHz, 1_{10}–1_{01} ground-state transition of ortho-H_2O toward VY Canis Majoris. In observations obtained with the *Submillimeter Wave Astronomy Satellite*, we measured a flux of ~450 Jy, in a spectrally resolved line centered on a velocity $v_{\rm LSR} = 25$ km s^{-1} with an FWHM of ~35 km s^{-1}, somewhat dependent on the assumed line shape. We analyze the line shape in the context of three different radial outflow models for which we provide analytical expressions. We also detected a weaker 557 GHz emission line from W Hydrae. We find that these and other H_2O emission-line strengths scale as suggested by Zubko and Elitzur.

Subject headings: circumstellar matter — infrared: stars — stars: individual (VY Canis Majoris, W Hydrae) — stars: mass loss — stars: winds, outflows

1. INTRODUCTION

VY Canis Majoris is a highly luminous, variable supergiant. It is strongly obscured; only 1% of the total luminosity is detected at optical wavelengths. The line-of-sight optical depths to the star at wavelengths of 1.65, 2.26, and 3.08 μm are 1.86 ± 0.42, 0.85 ± 0.20, and 0.44 ± 0.11 (Monnier, Geballe, & Danchi 1999). Correspondingly, the star exhibits a huge infrared excess. The star's distance is believed to be $D = 1500$ pc, implying a luminosity $L = 5 \times 10^5\ L_\odot$ (Lada & Reid 1978 and Richards, Yates, & Cohen 1998). A high signal-to-noise ratio infrared spectrum shows the star enveloped in an optically thick dust cloud whose inner edge is at a temperature of several hundred degrees (Harwit et al. 2001, hereafter Paper I). At greater distances from the star, the spectrum is dominated by amorphous silicate features.

Strong outflows have been reported by Buhl et al. (1975), who detected thermal emission in the vibrational ground-state ($v = 0$, $J = 2$–1) 86.84686 GHz SiO line. Reid & Dickinson (1976) interpreted these in terms of a stellar radial velocity of 17.6 ± 1.5 km s^{-1} with respect to the local standard of rest and an expansion velocity of 36.7 ± 2.0 km s^{-1}. Three thermally emitted mid-infrared water vapor emission lines seen in high-resolution spectra obtained with the Short Wavelength Spectrometer (SWS) on the *Infrared Space Observatory* (*ISO*) indicate a mean radial velocity of order 20 ± 2 km s^{-1} and a 25 km s^{-1} outflow velocity (Neufeld et al. 1999). These water vapor outflow velocities are significantly lower than the velocities for SiO cited by Reid & Dickinson (1976) or the 32 km s^{-1} velocities that Reid & Muhleman (1978) reported for 1612 MHz OH maser outflow.

The effective temperature of the central star appears to be $T_* = 2800$ K (Monnier et al. 1999). The combination of effective temperature, distance, and inferred luminosity fixes the star's radius at $R_* \sim 15$ AU. In the near-infrared at 0.8, 1.28, and 2.17 μm, VY CMa appears embedded in an elongated circumstellar envelope with respective dimensions of 60 × 83, 80 × 166, and 138 × 205 mas (Wittkowski, Langer, & Weigelt 1998). Working at 11 μm, Danchi et al. (1994) reported a variable photospheric radius ranging from 9.5 to 11 mas, where 10 mas corresponds to a stellar radius of 15 AU; the surrounding dust shell had a corresponding inner radius of 40–50 mas and an outer radius of 2.″5.

To model the dust disk surrounding VY CMa, Efstathiou & Rowan-Robinson (1990, hereafter ERR) assumed that the central star is orbited by a massive dusty disk, which flares out from the star at angles ±45° above and below the disk's central plane. At angles greater than 45° off the plane, radiation escapes into space. ERR believe that the line of sight from Earth is inclined at about 43° to the disk's orbital plane, so that we are looking almost tangentially through the outer layers of the disk. This radiative transfer model has been widely accepted because it accounts for the dust spectrum, the high reddening, and the lack of visible radiation from the star. However, as Ivezić & Elitzur (1995) have emphasized, a correct model must self-consistently couple the equations of radiative transfer to the outflow dynamics. Zubko & Elitzur (2000, hereafter ZE) have recently carried out such a calculation and used it to extensively model the semiregular M7.5 red giant W Hydrae.

In this Letter we reexamine the outflow problem. In § 2 we present new data on the strength and shape of the 557 GHz water vapor line observed with *SWAS* in VY CMa and W Hya. In § 3 we introduce complementing *ISO* data. In § 4 we attempt to model the geometry of the VY CMa outflow, while in § 5 we portray its radial dependence. In § 6 we summarize our findings.

2. OBSERVATIONS

In the course of many hundreds of *SWAS* orbits, between 1999 November and 2000 May, we carried out observations on VY CMa in the 556.936 GHz 1_{10}–1_{01} ground-state transition of ortho water vapor. All observations reported here were made with the spacecraft in the nodding mode (Melnick et al. 2000), with the telescope's primary field of view centered on $\alpha(2000) = 07^{\rm h}22^{\rm m}58.^{\rm s}3$, $\delta(2000) = -25°46'03.''0$. The observing time accumulated on-source was 7902 minutes (131.7 hr) with an equal time devoted to a blank field displaced south in declination by 0.°24.

The observed water vapor line, shown as a histogram in

[1] Also at Cornell University.

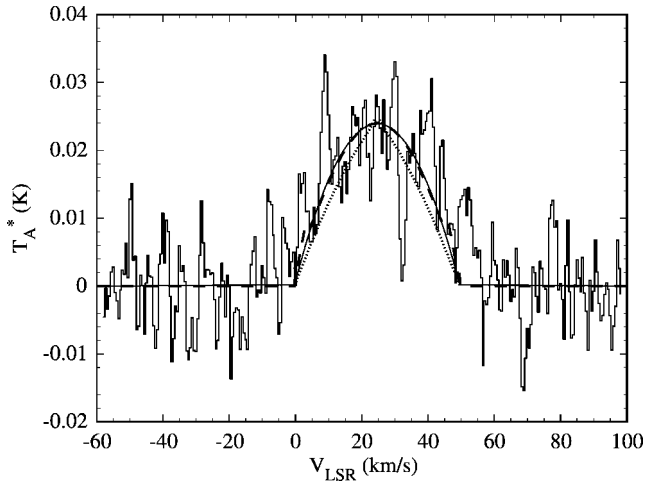


FIG. 1.—The 557 GHz water vapor spectrum of VY CMa obtained with *SWAS*. The histogram gives the *SWAS* observations. The solid line is a fit for a spherically symmetric outflow (model A). The dashed line is for a disk viewed edge-on [model (A−B)]; the dotted curve is a fit for the ERR outflow [model (A−C)]. All three curves are normalized to the observed line profile (see text and Fig. 2 for details).

Figure 1, is centered at 556.89 GHz, corresponding to a velocity with respect to the local standard of rest $v_{LSR} = 25$ km s^{-1}. A fit to the line shape discussed in § 4 yields an FWHM of ~35 km s^{-1}; the peak signal-to-noise ratio is 7. The area under the fit divided by its FWHM yields an antenna temperature $T_A^* = 0.033 \pm 0.005$ K ~ 450 Jy.

Using a beam centered on $\alpha(2000) = 13^h49^m02^s.1$, $\delta(2000) = -28°22'03''.0$, we carried out observations on W Hya in 1999 January and February, 1999 July, 2000 July, and 2001 February for a total of 126.7 hr, and we also detected the 557 GHz line. The antenna temperature was $T_A^* = 0.016 \pm 0.004$ K with a line width ~10.4 ± 2.1 km s^{-1}.

3. COMPLEMENTARY WATER VAPOR DATA

Neufeld et al. (1999) reported line strengths for more than 40 thermal water vapor emission lines from VY CMa observed with *ISO*, in the wavelength range of ~30–45 μm. Three transitions, respectively at 29.84, 31.77, and 40.69 μm, were also observed with SWS in its Fabry-Perot mode and exhibited P Cygni profiles and emission lines peaked at an average velocity of v_{LSR} ~ 20 km s^{-1}, consistent with the *SWAS* observations obtained at a higher velocity resolution of ~1 km s^{-1}. The outflow velocity of ~25 km s^{-1} inferred by Neufeld et al. (1999) is also in reasonable agreement with our 557 GHz results. The line profile obtained with *SWAS* does not exhibit P Cygni profiles, nor would we expect it to because the continuum is too weak to be detected. Archival *ISO* data obtained with the Long Wavelength Spectrometer (LWS) provide additional flux levels for transitions at 66.44, 108.078, 174.62, and 179.53 μm. Table 1 compares these data on VY CMa to measurements on W Hya compiled by ZE and found to be in reasonably good agreement with their theoretical model for the star. The table shows the flux levels in VY CMa and W Hya to be approximately in the ratio 10 : 1. The VY CMa data scaled down by a factor of 10 correspond well to the ZE model. Table 2 lists the characteristics of the two stars.

4. MODELING THE VY CMa OUTFLOW

The outflow from red supergiants is generally assumed to be propelled by radiatively accelerated dust grains that transfer their momentum to ambient gas. The VY CMa mass-loss rates cited by different observers range from ~ 1 to 3 × 10^{-4} $M_\odot$ yr^{-1} (see Paper I for a summary). The water vapor outflow can be expected to be roughly 1% of this by mass, and, given the high Einstein coefficient for the 557 GHz transition, $A = 3.45 \times 10^{-3}$ s^{-1}, the observed emission has to be optically thick. Velocity gradients, however, permit the radiation to escape, otherwise we would see only a velocity component from the approaching part of the outflow rather than from its entirety.

Despite the disk-shaped outflow postulated by ERR, the structure of the cloud surrounding VY CMa is quite uncertain. Planetary nebulae often light up bipolar flows that may have been ejected during a previous evolutionary phase. Figure 2*a* provides coordinates for an axially symmetric outflow whose axis of symmetry is inclined toward the observer at an angle θ_0. A spherically symmetric, constant velocity, optically thick outflow (model A) would yield a parabolic line shape shown as the solid curve in Figure 2*b*.

For the biconical geometry shown in Figure 2*a*, the flow directed at angle θ to the observer's line of sight is radially outward from the origin and describes a circular arc of radius $aa' = aa''$. Its length l spans points a' and a'' on a circle defined by the angle θ_0, by the opening angle α of the cone, and by the tilt angle toward the observer, θ, of the conical surface joining the origin to points on the circular arc. The length of

TABLE 1

RELATIVE o-H_2O FLUX LEVELS FROM VY CMa AND W HYA

Wavelength (μm)	Transition	W Hya[a] ($\times 10^{-20}$ W cm^{-2})	Model[b] ($\times 10^{-20}$ W cm^{-2})	VY CMa[c] ($\times 10^{-19}$ W cm^{-2})
538.289	$1_{10} \rightarrow 1_{01}$	0.45	0.76	0.34
179.527	$2_{12} \rightarrow 1_{01}$	8.66	12.48	8.7
174.624	$3_{03} \rightarrow 2_{12}$	9.21	8.31	8.8
108.073	$2_{12} \rightarrow 1_{10}$	13.00	15.47	13.2
66.438	$3_{30} \rightarrow 2_{21}$	22.90	18.45	17.2
40.691[d]	$4_{32} \rightarrow 3_{03}$	23.00	36.07	36.9
31.772[d]	$4_{41} \rightarrow 3_{12}$	63.0	39.95	24.1
29.837	$7_{25} \rightarrow 6_{16}$	32.00	30.72	23.5

[a] *ISO* data from Neufeld et al. 1996 and Barlow et al. 1996; *SWAS* data from this Letter.
[b] W Hya model from ZE, and 538 μm flux from V. Zubko & M. Elitzur 2001, private communication.
[c] For sources of data, see text.
[d] Blending may need to be taken into account.

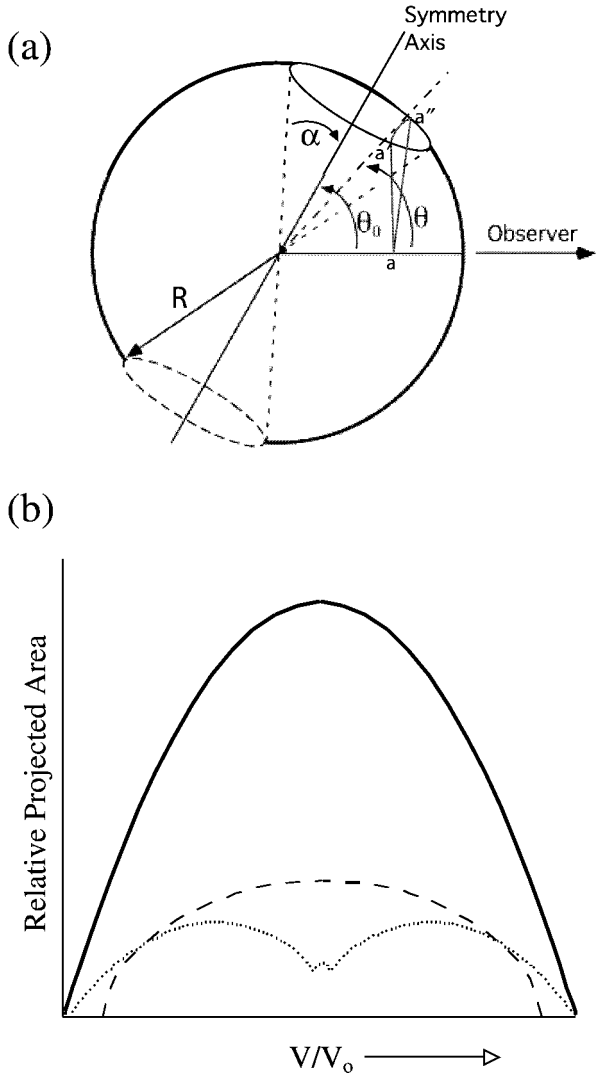


FIG. 2.—(*a*) Geometry of the outflow for which the velocity profiles were derived. *R* is the radius of a sphere whose radial extent is that of the outflow. For a biconical or disk-shaped flow, the angle θ_0 gives the tilt angle toward the line of sight. Throughout, we assume for simplicity that the symmetry axis and the line of sight define a plane of mirror symmetry in the outflow. The angle α is the opening angle of the conically shaped flow as measured from the symmetry axis. The angle θ defines the radial direction of motion of a volume in the flow relative to the line of sight to the observer. Points *a*, *a*′, and *a*″ lie in the plane of the sky. (*b*) The solid curve gives the expected line shape from a spherical outflow (model A). The dashed curve gives the expected line shape for a biconical outflow (model B) with $\theta_0 = 90°$ and $\alpha = 60°$, while the dotted line (model C) gives the line shape for an inclined biconical outflow with $\theta_0 = 47°$ and $\alpha = 45°$. Subtracting the biconical outflows from that for spherical outflows yields, respectively, the dashed and dotted line profiles for disk-shaped outflows in Fig. 1 (see text for details).

the arc, *l*, can be expressed as

$$l = R \sin\theta[\pi - 2 \sin^{-1}(\{\sin(\theta_0 - \alpha) + [\cos(\theta_0 - \alpha) - \cos\theta] \cot\theta_0\}/\sin\theta)]. \quad (1)$$

The segment formed by joining the origin to points along this arc presents to the observer a pie-shaped area projected on the plane of the sky, of measure $(Rl \sin\theta)/2$ defined by points *a*, *a*′, and *a*″. The projected velocity along the observer's line of sight throughout this surface is $v = v_0 \cos\theta$; for an optically thick line, the velocity distribution yielding the line shape is given by the relative values of $(Rl \sin\theta)/2$ at different angles $\theta = \cos^{-1}(v/v_0)$.

TABLE 2

CHARACTERISTICS OF VY CMa AND W HYA

Parameter	VY CMa[a]	W Hya[b]
Distance (pc)	1500	115
Luminosity ($L_\odot$)	5×10^5	11,050
Temperature (K)	2800	2500
Radius (cm)	2.25×10^{14}	3.9×10^{13}
Final outflow velocity (km s^{-1})	20	10
Optical depth[c]	$A_J \sim 3.2$	0.83 at 5500 Å
Gas-to-dust ratio	~100	850
Mass-loss rate ($M_\odot$ yr^{-1})	$\sim 2 \times 10^{-4}$	2.3×10^{-6}

[a] Data from Neufeld et al. 1996 and Barlow et al. 1996.
[b] For sources of data, see text.
[c] A_J is the optical depth in the *J* band.

An optically thick, biconical, constant-velocity outflow, symmetric about an axis perpendicular to the observer's line of sight (i.e., with $\theta_0 = \pi/2$) and limited to angles less than $\alpha = \pi/3$ from the axis of symmetry—with a density independent of angular distance from the axis (model B)—yields a line profile shown by the dashed curve in Figure 2*b*. A uniform biconical outflow within an angle of $\alpha = \pi/4$ from the axis, and with $\theta_0 = 47°$ (model C), would yield the bilobed dotted line shape shown in Figure 2*b*. Neither of these two models produces the line shape observed.

To obtain the line profile for an optically thick disk, we subtract these respective biconical outflows from a spherical outflow. For a disk with an axis perpendicular to the line of sight to the Earth, and a latitude-independent outflow into a disk with half-angle $\pm 30°$ above and below the symmetry plane, we can subtract the dashed curve in Figure 2*b* from the solid curve—i.e., model (A−B)—to obtain the fit shown by the dashed line in Figure 1. The line shape expected from the model proposed by ERR, equivalent to model (A−C), would result from a subtraction of the dotted line in Figure 2*b* from the solid curve. Figure 1 shows that models A and (A−B), normalized to the line strength and width, give rather better fits to the observed 557 GHz profile than does the ERR model (A−C).

5. THE TEMPERATURE/RADIUS PROFILE

ZE have devised the most comprehensive computational model of outflow developed to date from highly evolved stars. It derives a profile for temperature *T* and radial distance *R* from the star, $T^2R \sim$ constant. The gas in the outflow is primarily heated through collisions with grains, cooled by H_2O emission and adiabatic expansion, and effectively acts as though it was in thermal balance with the parent star throughout the flow. In apparent agreement with the general scaling properties proposed by Ivezić & Elitzur (1997) as applied to dusty gaseous outflows, Table 1 shows the good fit of the ZE model to the observed H_2O line strengths in W Hya that also scales well to VY CMa.

Given this observed agreement, we adopt the ZE profile, $T^2R =$ constant, for VY CMa. Paper I suggests the existence of a dust photosphere at a temperature $T_p \sim 400$ K in thermal equilibrium with the star. R_p is a characteristic radius for this photosphere in thermal balance with the star, $R_p^2 T_p^4 = R_*^2 T_*^4$, so that the ZE profile can be taken to extend all the way to the stellar surface: $T^2R = T_*^2 R_*$. In Table 3, we list the radial

TABLE 3

ORTHO-H_2O EMISSION: CHARACTERISTIC DISTANCES AND TEMPERATURES

Wavelength (μm)	Flux (Jy)	Radius[a] ($\times 10^{16}$ cm)	Temperature[a] (K)	T_u[b] (K)	T_l[b] (K)
538.289	450	8.1	148	60.95	34.23
179.527	3490	7.3	155	114.35	34.23
174.624	3440	7.2	156	196.72	114.35
108.073	3190	6.9	160	194.05	60.95
66.438	2560	1.6	332	410.55	194.05
40.691[c]	3360	0.99	431	550.30	196.72
31.772[c]	1710	0.45	626	702.21	249.37
29.837	1570	0.39	672	1125.55	643.34

[a] Derived from constancy of $TR^{1/2}$ (see text).
[b] Level energies divided by Boltzmann constant.
[c] Blending may need to be taken into account.

distances at which the VY CMa water vapor lines emanate, on the assumption that the emitting region is optically thick—an assumption justified by the deep P Cygni profiles of even the highest rotational lines observed. The flux received from a circumstellar cloud subtending a solid angle Ω at the observer is then

$$F(\nu) = \frac{2\nu^2 kT}{c^2}\,\Omega = \frac{2kT}{\lambda^2}\frac{R^2}{D^2}\,\psi, \tag{2}$$

where we assume that all the radiation is in the Rayleigh-Jeans part of the spectrum. Table 3 shows this assumption to be consistent; D is the distance to the star, R is the radial distance of the emitting H_2O region from the star, and ψ is a constant of order unity that depends on the geometry of the outflow. It has a higher value for a sphere than for a flattened disk. Table 3 assumes $\psi \sim 1$. Substituting for the stellar parameters $T_* = 2800$ K, $R_* = 2.25 \times 10^{14}$ cm, and $D = 4.5 \times 10^{21}$ cm and taking the emission to be blackbody in the frequency interval observed, we can solve for the characteristic distances from the central star and the corresponding temperatures at which the different spectral lines appear to be emitted:

$$R = \left[\frac{1.75 \times 10^{25} F(\nu)\lambda^2}{\psi}\right]^{2/3}, \tag{3}$$

where $F(\nu)$ is given in janskys and where R and λ both are in units of centimeters. The calculated distances for the last three lines in Table 3 use the full emission-line strengths corrected for P Cygni absorption of the continuum. For the longer wavelength lines observed with the *ISO* LWS, the resolution is insufficient to determine whether self-absorption weakened the lines.

6. CONCLUSIONS

We have obtained a high-resolution spectrum of the 557 GHz water vapor emission line from the circumstellar cloud surrounding VY CMa, and we have obtained a weaker signal from W Hya. The observed flux for VY CMa is ~450 Jy. The line shape is symmetric around a recession velocity $v_{\rm LSR} = 25$ km s^{-1} and has an FWHM of order ~35 km s^{-1}. We have developed analytical line fits for several plausible models of the outflow. Observations that will be possible with the *Herschel Space Observatory* should yield improved line shapes that will further constrain outflow models. Archival and published *ISO* data for VY CMa and W Hya suggest the adoption of a model developed by ZE to determine the distance from the central star and the temperature regime around VY CMa from which the H_2O lines emanate.

We have been supported by contract NAS-30702 from NASA for work on the *Submillimeter Wave Astronomy Satellite* and contract NASA/JPL 1203030 for work on the *Infrared Space Observatory*. We thank Gary Melnick and David Neufeld for critically reading our manuscript, the referee Keiichi Ohnaka for thoughtful and incisive comments, and Viktor Zubko and Moshe Elitzur for their results of unpublished calculations.

REFERENCES

Barlow, M. J., et al. 1996, A&A, 315, L241
Buhl, D., Snyder, L. E., Lovas, F. J., & Jonson, D. R. 1975, ApJ, 201, L29
Danchi, W. C., Bester, M., Degiacomi, C. G., Greenhill, L. J., & Townes, C. H. 1994, AJ, 107, 1469
Efstathiou, A., & Rowan-Robinson, M. 1990, MNRAS, 245, 275 (ERR)
Harwit, M., Malfait, K., Decin, L., Waelkens, C., Feuchtgruber, H., & Melnick, G. J. 2001, ApJ, 557, 844 (Paper I)
Ivezić, Ž., & Elitzur, M. 1995, ApJ, 445, 415
———. 1997, MNRAS, 287, 799
Lada, C. J., & Reid, M. J. 1978, ApJ, 219, 95
Melnick, G. J., et al. 2000, ApJ, 539, L77
Monnier, J. D., Geballe, T. R., & Danchi, W. C. 1999, ApJ, 512, 351
Neufeld, D. A., Chen, W., Melnick, G. J., de Graauw, T., Feuchtgruber, H., Haser, L., Lutz, D., & Harwit, M. 1996, A&A, 315, L237
Neufeld, D. A., Feuchtgruber, H., Harwit, M., & Melnick, G. J. 1999, ApJ, 517, L147
Reid, M. J., & Dickinson, D. F. 1976, ApJ, 209, 505
Reid, M. J., & Muhleman, D. O. 1978, ApJ, 220, 229
Richards, A. M. S., Yates, J. A., & Cohen, R. J. 1998, MNRAS, 299, 319
Wittkowski, M., Langer, N., & Weigelt, G. 1998, A&A, 340, L39
Zubko, V., & Elitzur, M. 2000, ApJ, 544, L137 (ZE)